DMD Fast Forward. Published on November 6, 2012 as doi:10.1124/dmd.112.048918
This article has not been copyedited and formatted. The final version may differ from this version.

In Vitro Investigations into the Roles of Drug Transporters and Metabolizing Enzymes in the Disposition and Drug Interactions of Dolutegravir, a HIV Integrase Inhibitor

Melinda J. Reese, Paul M. Savina, Grant T. Generaux, Helen Tracey, Joan E. Humphreys, Eri Kanaoka, Lindsey O. Webster, Kelly A. Harmon, James D. Clarke and Joseph W. Polli

Drug Metabolism and Pharmacokinetics, GlaxoSmithKline, Research Triangle Park, NC USA (MJR, PMS, GTG, JEH, LOW, KAH, JWP)

Drug Metabolism and Pharmacokinetics, GlaxoSmithKline, Ware, UK (HT, JDC)

Shionogi Research Laboratories, Shionogi & Co., Ltd., Osaka, Japan (EK)

DMD Fast Forward. Published on November 6, 2012 as DOI: 10.1124/dmd.112.048918
This article has not been copyedited and formatted. The final version may differ from this version.

Running Title: In Vitro Investigations with Dolutegravir

* To whom correspondence should be addressed.

Melinda J Reese

Preclinical Drug Metabolism and Pharmacokinetics

GlaxoSmithKline, Inc.

Room: 2.4075.1

Research Triangle Park, NC 27709

Phone: (919) 483-4077

FAX: (919) 315-6003

Email: mindy.j.reese@gsk.com

Number of Text Pages: 24

Number of Tables: 3

Number of Figures: 4

Number of references: 60

Word Count:

Abstract: 236

Introduction: 660

Discussion: 1500

DMD Fast Forward. Published on November 6, 2012 as DOI: 10.1124/dmd.112.048918
This article has not been copyedited and formatted. The final version may differ from this version.

Nonstandard abbreviations: ABC = ATP-binding cassette; A→B = Apical to basolateral; BCRP = human breast cancer resistance protein; B→A = Basolateral to apical; B→A/A→B ratio = $P_{app\ B\rightarrow A}/P_{app\ A\rightarrow B}$; BNF = β-naphthoflavone; CHO = Chinese hamster ovary cell line; CL_i = intrinsic clearance; CYP = cytochrome P450; DTG= dolutegravir (S/GSK1349572; (4*R*,12a*S*)-*N*-(2,4-Difluorobenzyl)-7-hydroxy-4-methyl-6,8-dioxo-3,4,6,8,12,12a-hexahydro-2*H*-pyrido[1',2':4,5]pyrazino[2,1-*b*][1,3]oxazine-9-carboxamide}; DDI = drug-drug interaction; EG = estradiol 17β-D-glucuronide; FaSSIF = fasted state simulated intestinal fluid; F_g = fraction of drug escaping intestinal metabolism; fm = fraction metabolized; fu = fraction unbound in plasma; HFC = 7-hydroxy-4-(trifluoromethyl) coumarin; HEK= human embryonic kidney cells; HLM = human liver microsomes; IC_{50} = concentration required for 50% inhibition; INI = integrase inhibitor; K = inhibitor concentration required for 50% increase in the cimetidine A → B rate; K_i = inhibition constant; K_{inact} = maximum inactivation rate; K_I = concentration producing half the maximal inactivation rate; k_{deg} = rate constant for hepatic CYP enzyme degradation; K_m = concentration at half-maximal rate; LSC = liquid scintillation counting; MDCK = Madin Darby canine kidney cells; MDI = metabolism-dependent inhibition; MRP2 = multidrug resistance associated protein-2 transporter; NNRTI = non nucleoside reverse transcriptase inhibitor; NRTI = nucleoside or nucleotide reverse transcriptase inhibitor; OATP = organic anion transporting polypeptide; OCT = organic cation transporter; PB = phenobarbital; P_{app} = apparent permeability; Pgp = P-glycoprotein; PI = protease inhibitors; PXR = pregnane X receptor; RIF = rifampicin; SLC = solute carrier; UGT = UDP glucuronosyltransferase; UDPGA = UDP glucuronic acid; Vd = volume of distribution; V_{max}= maximum rate of metabolism

DMD Fast Forward. Published on November 6, 2012 as DOI: 10.1124/dmd.112.048918
This article has not been copyedited and formatted. The final version may differ from this version.

Abstract

Dolutegravir (DTG; S/GSK1349572) is a potent HIV-1 integrase inhibitor with a distinct resistance profile and a once daily dose regimen that does not require pharmacokinetic boosting. This work investigated the in vitro drug transport and metabolism of DTG and assessed the potential for clinical drug-drug interactions. DTG is a substrate for the efflux transporters P-glycoprotein (Pgp) and Breast Cancer Resistance Protein (BCRP). Its high intrinsic membrane permeability limits the impact these transporters have on DTG's intestinal absorption. UDP-glucuronosyltransferase (UGT) 1A1 is the main enzyme responsible for the metabolism of DTG in vivo, with cytochrome P450 (CYP) 3A4 being a notable pathway and UGT1A3 and UGT1A9 being only minor pathways. DTG demonstrated little or no inhibition (IC_{50} values > 30 μM) in vitro of the transporters Pgp, BCRP, multidrug resistance protein (MRP) 2, organic anion transporting polypeptide (OATP) 1B1/3, organic cation transporter (OCT) 1, or the drug metabolizing enzymes CYP1A2, 2A6, 2B6, 2C8, 2C9, 2C19, 2D6, 3A4, UGT1A1 or 2B7. Further, DTG did not induce CYP1A2, 2B6, or 3A4 mRNA in vitro using human hepatocytes. DTG does inhibit the renal OCT2 (IC_{50} = 1.9 μM) transporter, which provides a mechanistic basis for the mild increases in serum creatinine observed in clinical studies. These in vitro studies demonstrate a low propensity for DTG to be a perpetrator of clinical drug interactions, and provide a basis for predicting when other drugs could result in a drug interaction with DTG.

Introduction

Today, the treatment of Human Immunodeficiency Virus (HIV)-1 infection incorporates multiple agents into combination antiretroviral therapy that targets different phases of the HIV life cycle. The Department of Health and Human Services Guidelines for the Use of Antiretroviral Agents in HIV-1-Infected Adults and Adolescents recommends various combination-based regimens that consist of drugs from classes that include: nucleoside reverse transcriptase inhibitors (NRTIs), non-nucleoside reverse transcriptase inhibitors (NNRTIs), protease inhibitors (PIs), integrase inhibitor (INIs), or C-C chemokine receptor type 5 (CCR5) antagonists [Panel on Antiretroviral Guidelines for Adults and Adolescents, 2012]. The impact of combination therapy (e.g., highly active antiretroviral therapy; HAART) has resulted in very low to undetectable HIV RNA in serum, patients living longer and fewer dying from the disease [Palella et al., 1998;Palella et al., 2006]. This outcome changes the focus of HIV therapy from one mainly focused on managing the viral disease to one of also considering other co-morbidities, including the treatment of an aging HIV population with conditions such as cardiovascular disease and diabetes. Thus, as newer HIV agents come to market, the drug-drug interaction (DDI) assessment needs to include a broader number of co-medications than previously considered for the treatment of HIV disease.

Management of DDIs in HIV subjects is challenging because the major mechanisms of DDIs in antiretroviral combination therapy involve CYP enzymes, ATP-binding cassette efflux transporters, and solute carrier uptake transporters [Zembruski et al., 2011a]. Most PIs (e.g. lopinavir, fosamprenavir, darunavir) are substrates or inhibitors of CYP3A4, and many of these agents require boosting with ritonavir, a very potent CYP3A4 inhibitor [Hull and Montaner,

2011]. Inhibition of metabolic enzymes is not limited to only PIs or the CYP enzyme family, but other antiviral drugs such as atazanavir are potent inhibitors of both CYP3A4 and UDP-glucuronosyltransferase 1A1 (UGT1A1) [Zhang et al., 2005]. Enzyme inhibition is not the only DDI concern, as potent CYP3A4 inducers, such as NNRTIs etravirine and efavirenz, can increase the metabolism of co-administered drugs resulting in reduced exposure and efficacy [Yanakakis and Bumpus, 2012;Hariparsad et al., 2004]. Finally, to add to the complexity, a single agent such as ritonavir can simultaneously be a potent inhibitor of one pathway (e.g., CYP3A4) and a potent inducer for another (e.g., CYP2C19) [Yeh et al., 2006].

In addition to metabolic enzymes, drug transporters can influence antiviral drug disposition. Protease inhibitors are transported by efflux transporters such as Pgp, BCRP and MRP2 and the OATP uptake transporters [Dixit et al., 2007]. Co-administration of Pgp or BCRP inhibitors, such as ritonavir or saquinavir, may increase the oral absorption of an HIV co-medication that is a substrate for these transporters, or allow entry into more restricted tissues such as the brain or placenta. Alternatively, absorption can be reduced via induction of these transporters. Clinically significant Pgp interactions have been reported with the protease inhibitors tipranavir/ritonavir and the Pgp substrate loperamide resulting in a 50% reduction in the AUC of loperamide [Mukwaya et al., 2005].

Dolutegravir (DTG) is a tricyclic carbamoyl pyridone integrase inhibitor (INI) that blocks the strand transfer step during the integration of the HIV-1 DNA into the genome of the host cell. The unique features of DTG include a superior resistance profile and once daily low milligram dosing that does not require pharmacokinetic boosting [Min et al., 2010]. Like other

antiretroviral agents, it is expected that DTG will be co-administered in combination with a wide variety of other drugs, including agents other than antivirals for non-HIV related co-morbidities. Because of the potential overlapping transporter and metabolic pathways of DTG and drugs co-administered to treat HIV infection or other diseases, it is critical to evaluate the potential for clinical DDIs, especially in the HIV polypharmacy setting. Therefore the objective of this study was to investigate the mechanisms for the potential role of transporters and metabolizing enzymes in the disposition of DTG, to provide a basis for predicting when other drugs could result in a drug interaction with DTG, and when DTG might cause interactions with other co-administered drugs.

Materials and Methods

Materials. GlaxoSmithKline Active Pharmaceutical Ingredient Chemistry and Analysis (Stevenage, UK) supplied [^{14}C]DTG (59 mCi/mmol), GF120918 (Elacridar), and [^{14}C]cimetidine (57 mCi/mmol). [^{3}H]Digoxin (5 Ci/mmol) and [^{3}H]amprenavir (19 Ci/mmol) were purchased from GE Healthcare/Amersham Biosciences (Piscataway, NJ). [^{3}H]Estradiol 17β-D-glucuronide (EG; 50 Ci/mmol) was purchased from Perkin Elmer (Boston, MA). Cryopreserved human hepatocytes (pool of 3 donors; 2 male and 1 female) were obtained from Cellzdirect (Durham, NC). Pooled human liver microsomes (prepared from 15 donors) were obtained from Xenotech LLC (Lenexa, KS), and the microsomal protein concentration and CYP content were provided by the manufacturer. Supersomes™, containing individually over-expressed human UGT or CYP enzymes, or vector control membranes, derived from baculovirus infected insect cells were obtained from BD Gentest (Woburn, MA). Cell culture reagents were purchased from Invitrogen (Carlsbad, CA). Transwells (12-well, 11-mm diameter, 0.4 μm pores) were purchased from Corning Costar (Cambridge, MA). All other reagents were HPLC or analytical grade.

Monolayer Efflux Studies. The polarized Madin-Darby canine kidney (MDCKII) cells heterologously expressing either human Pgp or BCRP were used for the in vitro transport studies and were obtained from the Netherlands Cancer Institute (Amsterdam, Netherlands). Cell culture and transport studies were completed as previously described [Polli et al., 2008]. Stock solutions of [^{14}C]DTG, GF120918 (a Pgp and BCRP inhibitor), and the positive control substrates [^{3}H]amprenavir (Pgp substrate) and [^{14}C]cimetidine (BCRP substrate) were prepared in DMSO. The transport of [^{14}C]DTG and positive control substrates was measured in two

DMD Fast Forward. Published on November 6, 2012 as DOI: 10.1124/dmd.112.048918
This article has not been copyedited and formatted. The final version may differ from this version.

directions (apical to basolateral [A→B] and basolateral to apical [B→A]). DTG was tested in triplicate (0.3 to 100 μM). The passive membrane permeability of [^{14}C]DTG (3 μM) was determined as described previously [Polli et al., 2001;Polli et al., 2008] at pH 7.4/7.4 in Dulbecco's Modified Eagle Medium (both donor and receiver sides), and at pH 5.5/7.4 or 7.4/7.4 using a bio-relevant buffer (FaSSIF, fasted state simulated intestinal fluid on the donor side and 1% human serum albumin on the receiver side) to simulate conditions in the gastrointestinal tract; pH 5.5 was selected as the lower pH because it provides a larger pH range that is reflective of the variability observed in the human and animal gastrointestinal tract [Evans et al., 1988;Lui et al., 1986]. The passive membrane permeability was determined in the presence of 3 μM GF120198, which was used to inhibit efflux pumps, and Lucifer yellow was included to verify monolayer integrity. . Drugs were quantified by liquid scintillation counting (LSC) using a TriCarb T2900 liquid scintillation counter and Ultima Gold scintillation cocktail (Perkin Elmer, Boston, MA).

Pgp and BCRP Inhibition Assays. Cell culture and transport studies were completed as described previously [Polli et al., 2008;Rautio et al., 2006]. Experiments were conducted for 90 min using [^{3}H]digoxin (27 nM) as the probe substrate for Pgp and [^{14}C]cimetidine (80 nM) for BCRP. DTG was tested in triplicate (0.3 to 100 μM). [^{3}H]Digoxin and [^{14}C]cimetidine were quantified by LSC. GF120918 was used as positive control inhibitor for both Pgp and BCRP.

MRP2 Inhibition Assays. DTG and its glucuronide metabolite (M2) were evaluated for inhibition of the multidrug resistance associated protein-2 transporter (MRP2) in vitro using the probe substrate [^{3}H]EG and membrane vesicles prepared from baculovirus infected Sf9 cells

DMD Fast Forward. Published on November 6, 2012 as DOI: 10.1124/dmd.112.048918
This article has not been copyedited and formatted. The final version may differ from this version.

expressing human MRP2 (Invitrogen, Carlsbad, CA). Vesicles (50 µg protein) were preincubated for 5 minutes at 37°C in reaction buffer with DTG or M2 (0.1 to 100 μM) or positive control benzbromarone (0.1 to 100 μM), and reactions initiated by the addition of 10 mM MgATP solution containing 50 µM [^{3}H]EG. Additional incubations were performed in the absence of inhibitor and in the presence of 10 mM MgAMP solution for passive transport. After 3 minutes, reactions were terminated by the addition of chilled stopping buffer (40 mM MOPS-Tris, 70 mM KCL) and samples transferred to 96-well glass fiber filter plates, washed, and radioactivity measured using LSC.

OATP Assays. For OATP1B1 studies, Chinese hamster ovary cell line heterologously expressing the human OATP1B1 transporter (CHO-OATP1B1) obtained from the University of Zurich was used. Human embryonic kidney (HEK) MSRII cells (American Type Culture Collection, Manassas, VA) transduced with BacMam baculovirus containing the human OATP1B3 transporter, were used for the OATP1B3 inhibition assay. Cell culture and inhibition studies were completed as described previously [Polli et al., 2008]. DTG was tested in triplicate (0.3 to 100 μM) and rifamycin SV (10 μM) was used as a positive control inhibitor.

OCT Inhibition Assays. OCT1 inhibition screening studies were conducted at Absorption Systems LP (Exton, PA) using HEK293 cells expressing OCT1. [^{14}C]Metformin (10µM) was incubated with DTG (10µM) or positive control inhibitor (10 µM repaglinide or 100 µM quinidine) for 10 minutes at 37°C in a humidified incubator. Incubations were performed in triplicate. Cells were lysed with 75% ethanol and radioactivity measured by LSC in a Tri-Carb 2900TR liquid scintillation analyzer (PerkinElmer). OCT2 inhibition studies were conducted at

Optivia (Menlo Park, CA). MDCK-II cells grown on permeable supports were transfected with a vector containing OCT2. The transport of [^{14}C]metformin (10μM) was determined by LSC. DTG was tested in triplicate (0.1 to 30 μM). Cimetidine was used as a positive control inhibitor (100 μM and 300 μM).

Identification of the Enzymes Involved in the Metabolism of Dolutegravir. [^{14}C]DTG (50μM) was incubated with pooled cryopreserved human hepatocytes (1.5 million cells/mL) in Weymouth's medium containing 5% fetal bovine serum for 4 and 20 hours at 37°C in a CO_2 incubator. Reactions were terminated with an equal volume of acetonitrile, samples centrifuged and supernatants analyzed by radio-HPLC. Incubations with media but no cells served as negative controls. Positive control incubations were performed with 7-ethoxycoumarin to confirm phase I and II metabolism of the hepatocytes. The effect of a selective CYP3A4 inhibitor, azamulin, on the metabolism of DTG was evaluated by pre-incubating azamulin (5μM) with HLM (2mg/mL), 0.1M phosphate buffer, pH 7.4, and cofactor for 10min before adding [^{14}C]DTG to start the reaction. Reactions were terminated after 2hr by adding an equal volume of acetonitrile. Control incubations were performed in the absence of azamulin, cofactor, or HLM. CYP reaction phenotyping experiments were conducted by pre-incubating Supersomes™ expressing individual human CYP enzymes, CYP1A2, 2B6, 2C8, 2C9, 2C19, 2D6, and 3A4 (150pmol/mL), for 5 min at 37°C with [^{14}C]DTG (5 μM) in 0.1M phosphate buffer, pH 7.4. Reactions were initiated with the addition of cofactor (an NADPH regenerating system consisting of 1 mM NADPH, 5.5 mM glucose-6-phosphate and 1.2 units/mL glucose-6-phosphate dehydrogenase) and terminated after 2hr by the addition of an equal volume of acetonitrile. Incubations were performed with no cofactor and with vector control membranes.

DMD Fast Forward. Published on November 6, 2012 as DOI: 10.1124/dmd.112.048918
This article has not been copyedited and formatted. The final version may differ from this version.

For UGT reaction phenotyping experiments HLM (1 mg/mL) were incubated with alamethicin (50 μg/mg microsomal protein), in 0.1M Tris-HCl, pH 7.4 buffer and 2mM $MgCl_2$ for 15min on ice. [^{14}C]DTG (16μM) was added to HLM for 5min at 37°C and reactions initiated with cofactor (5mM UDPGA). Incubations were performed, in duplicate, 0 to 4 hours. The effect of atazanavir, a UGT1A1 inhibitor [Zhang et al., 2005] on [^{14}C]DTG glucuronidation was evaluated in HLM preincubated with [^{14}C]DTG (10μM) and atazanavir (0.1 to 30μM) for 5 minutes. Reactions were initiated by cofactor and incubated for 2 hours. [^{14}C]DTG incubations with recombinant human UGT enzymes (UGT1A1, 1A3, 1A4, 1A6, 1A9, 2B4, 2B7, or 2B15; at 1mg/mL protein) were conducted by activating the enzymes with alamethicin as described above. Reactions were started with UDPGA and incubations performed for 2 and 4 hours. Control incubations were performed in the 1) absence of cofactor, and 2) with UGT insect cell control Supersomes™ (lacking UGT activity) (BD Gentest, Woburn, MA). The in vitro enzyme kinetic parameters were determined for glucuronide formation of [^{14}C]DTG (2.0, 5.0, 10, 25, 50, and 100 μM) in HLM and human UGT1A1 enzymes. Incubations were performed for 2 hours and processed as described previously.

HPLC Radiochemical profiling and metabolite identification.

Radiochemical profiles of human hepatocytes, HLM and recombinant CYP and UGT incubations were generated using an Agilent 1100 HPLC system (Palo Alto, CA, USA) coupled with a model 625 radiochemical detector (Perkin Elmer Life Sciences, Waltham MA, USA) equipped with a 0.5 mL flow cell. Chromatography was performed using a Symmetry C18 Symmetry (100 x 4.6 mm, 3.5 μm) analytical column (Waters, Milford, MA, USA) maintained

DMD Fast Forward. Published on November 6, 2012 as DOI: 10.1124/dmd.112.048918
This article has not been copyedited and formatted. The final version may differ from this version.

at a temperature of 40°C. The mobile phase consisted of two solvents: A (aqueous 0.1% ammonium acetate) and B (acetonitrile containing 0.1% ammonium acetate) delivered at a flow rate of 1.5 mL/minute. Separations were achieved by using a gradient profile: 0-3.3 min, 5% B; 3.3-40 min, 5-25% B; 40-43.3 min, 25-35% B; 43.3-46.7 min, 35-95% B; 46.7-48.3 min, 95% B and returned to initial conditions with a 10 min. equilibration between injections. For on-line detection, the ratio of scintillation fluid (Ultima Flo M) to mobile phase was 2:1. DTG metabolites were identified by LC-MS/MS using an Agilent 1100 HPLC System interfaced with a ThermoFinnigan LTQ-Orbitrap mass spectrometer (Thermo Corporation, San Jose, CA, USA), operated in positive ion, full scan, MS/MS or MSn modes with argon or helium as the collision gas. Leucine enkephalin (c.a. 0.1 µg/mL) was used as a lock mass for accurate mass measurements on the Q-Tof. The combination of retention time, accurate mass from the full scan and subsequent MS/MS or MSn scans, and comparison with spectroscopic data from other nonclinical studies (unpublished data) were used for structural identification of DTG and its metabolites.

CYP inhibition by Dolutegravir. The potential for DTG to inhibit human CYP enzymes (CYP1A2, 2A6, 2B6, 2C8, 2C9, 2C19, 2D6, and 3A4) in a direct and metabolism-dependent manner was evaluated in HLM (0.1 mg/mL). Incubation conditions, analytical details positive control inhibitors and specific probe substrates for the CYP inhibition studies were conducted as described [Polli et al., 2012]. Incubations for DTG and positive control inhibitors were tested in duplicate (0.1 to 100 μM). To assess direct CYP inhibition, reactions were initiated by an NADPH regenerating system (cofactor solution consisting of 1.7mg of $NADP^+$, 7.8mg of glucose-6-phosphate, and 6 units of glucose-6-phosphate dehydrogenase per mL). CYP

metabolism-dependent inhibition (MDI) was examined by pre-incubating DTG with HLM and cofactor for 20 minutes and continuing incubation with the individual probe substrate for 5-10 minutes. Reactions were terminated with a half volume of acetonitrile containing internal standard for the reference compound and centrifuged to remove protein. Supernatants were injected onto an Inertsil 33 x 3 mm ODS-3 3µM HPLC column (GL Sciences Inc, Torrance, CA) and analyzed by validated LC-MS/MS methods utilizing a Sciex API4000^{TM} (AppliedBiosystems/MSD Sciex, Ontario, Canada) equipped with an electrospray ionisation source (ESI) as described [Polli et al., 2012]. Analyte (probe substrate metabolite) to internal standard peak area ratios were calculated and the metabolite concentrations were determined by interpolation from the individual standard curve. Rates of metabolite production at each concentration were expressed as a percentage of the mean uninhibited control rate for each assay. Non-linear regression analysis of the data was performed using GraFit (v.5.0.8, Erithacus software, Limited, London) to calculate IC_{50} values.

UGT inhibition by Dolutegravir. The ability of DTG to inhibit UGT1A1 and 2B7 was evaluated by measuring the glucuronidation of scopoletin (20µM; UGT1A1) and 7-hydroxy-4-(trifluoromethyl) coumarin (HFC; 15µM; UGT2B7) in UGT Supersomes™ (BD Gentest, Woburn MA) using fluorescence detection [Collier et al., 2000]. DTG (0.1-100µM) or positive control inhibitor atazanavir (UGT1A1) or gemfibrozil (UGT2B7) was incubated in duplicate in a 96-well OptiPlate™ (Perkin Elmer) in a 0.1M Tris HCl pH 7.4 buffer containing 5mM $MgCl_2$, probe substrate, 25µg/mL alamethicin, and 0.25mg/mL UGT enzymes. Reactions were initiated by 2mM UDPGA. Sample analysis was performed using fluorescence detection with a SpectraMax M2^{e} microplate reader (Molecular Devices, Sunnyvale, CA). The decrease in

scopoletin or HFC fluorescence due to the production of the glucuronide metabolite was monitored at excitation and emission wavelengths of 410 and 590nm, respectively, with measurements taken every 2 min over the course of 30 min. Rates of scopoletin or HFC glucuronidation were calculated by monitoring a decrease in substrate fluorescence in the absence and presence of inhibitor and expressed as the rate (slope). Rates of metabolite production at each concentration of inhibitor were expressed as a percentage of the mean uninhibited control rate for each assay. The IC_{50} values were calculated using GraFit software.

Induction of CYP mRNA by Dolutegravir in Human Hepatocytes. Primary human hepatocytes from a single donor were obtained commercially plated in a sandwich configuration on a collagen substratum with Matrigel overlay (CellzDirect, Austin, TX); three separate donors were tested. Hepatocytes were treated for 2 days with DTG (1, 5, 10, 20, 30, and 40 μM), vehicle control (0.1% DMSO), or prototypical inducers, β-naphthoflavone (BNF; CYP1A2) (35μM), phenobarbital (PB; CYP2B6) (1mM) and rifampicin (RIF; CYP3A4) (20μM). Following culture and test compound treatment cells were lysed and total RNA extracted. mRNA expression for each CYP was determined using quantitative real-time polymerase chain reaction technology (TaqMan™) [Bowen et al., 2000]. Relative differences in mRNA expression were assessed based on different cycling threshold (Ct) values which were determined by the ABI 7900 Real Time PCR System Sequence Detection Software (SDS v1.3).

Calculations.

For monolayer efflux studies, the flux of DTG and probe substrates was calculated using the following equation:

$$J = \frac{V(\mathrm{d}C/\mathrm{d}t)}{A}$$

where J is the flux (nmol/cm^2/h), V is the receptor volume (mL), C is the receiver drug concentration (nmol/ml), t is time in hours, and A is the membrane surface area (cm^2).

The passive permeability of DTG, probe substrates and Lucifer yellow in the presence of GF120918 was determined using the following equation as described previously [Rautio et al., 2006]:

$$P_{7.4} = -\left(\frac{V_D V_R}{(V_D + V_R)At}\right)\ln\left\{1 - \frac{(V_D + V_R)C_R(t)}{(V_D C_D(t) + V_R C_R(t))}\right\} \text{ x } 10^7 \text{ nm/s}$$

where $P_{7.4}$ is the permeability coefficient at pH 7.4, V_D, V_R are donor and receiver well volumes, respectively (mL), A is the membrane surface area (cm^2), t is the incubation time (seconds), $C_R(t)$ is the measured concentration in the receiver well at time t (nmol/mL), $C_D(t)$ is the measured concentration in the donor well at time t (nmol/mL).

For transporter and CYP inhibition studies, the IC_{50} values (the concentration of inhibitor required for 50% inhibition of the monolayer transport, cellular uptake or metabolite production rates) were calculated with GraFit (version 5.08 Erithacus Software Limited, London, UK) using:

$$y = \frac{Range}{1 + \left(\frac{x}{IC_{50}}\right)^s} + \text{background}$$

where y = the rate of transport, uptake or metabolite generation of an appropriate probe (expressed as a percentage of the uninhibited control), *Range* = the rate in the absence of test

DMD Fast Forward. Published on November 6, 2012 as DOI: 10.1124/dmd.112.048918
This article has not been copyedited and formatted. The final version may differ from this version.

compound, *s* = the slope factor, *x* = the inhibitor concentration (µM), background = the uninhibited rate (expressed as a percentage of the total rate).

For UGT1A1 enzyme kinetic determinations non-linear regression analysis of the ether glucuronide formation was performed using GraFit. Michaelis-Menten parameters V_{max}, K_m, and CL_i were calculated using the following equations:

$$v = \frac{V_{\max}.[S]}{K_m + [S]} \qquad CLi = \frac{V\max}{Km}$$

Where V_{max} is maximal rate of metabolite produced, K_m is equal to the substrate concentration at which the reaction rate is half its maximal value, [S] is the substrate concentration, and CL_i is the intrinsic clearance.

In vitro-in vivo extrapolation of DTG as a victim of UGT1A1 and CYP3A4 inhibition

A mechanistic static equation based on previously described models [Hinton et al., 2008] was used to predict the magnitude of DTG exposure in vivo when co-administered with the clinically relevant UGT1A1 and CYP3A4 inhibitors, atazanavir and ritonavir:

$$\frac{AUCi}{AUC} = \frac{1}{\frac{fm_{CYP3A4}}{1+\frac{[I]_{ATZ}}{Ki_{ATZ,CYP3A4}}+\frac{[I]_{RTV}}{Ki_{RTV,CYP3A4}}} + \frac{fm_{UGT1A1}}{1+\frac{[I]_{ATZ}}{Ki_{ATZ,UGT1A1}}+\frac{[I]_{RTV}}{Ki_{RTV,UGT1A1}}} + (1 - fm_{CYP3A4} - fm_{UGT1A1})}$$

Unbound hepatic inlet concentrations of atazanavir, $[I]_{ATZ}$ (0.74 µM), and ritonavir, $[I]_{RTV}$ (0.016 µM), were estimated according to methods previously described in the literature [Ito et al., 1998]. The atazanavir inhibition constants for UGT1A1 and CYP3A4 are $K_{i,ATZ,UGT1A1}$ (0.2 µM) and $Ki_{,ATZ,CYP3A4}$ (2.35 µM) , respectively [Busti et al., 2004]. Ritonavir inhibition constants for

DMD Fast Forward. Published on November 6, 2012 as DOI: 10.1124/dmd.112.048918
This article has not been copyedited and formatted. The final version may differ from this version.

CYP3A4 and UGT1A1 are shown as $K_{i,RTV,3A4}$ (0.03 μM) and $K_{i,RTV,UGT1A1}$ (9.5 μM) [Granfors et al., 2006;Zhang et al., 2005]. The $K_{i,RTV,UGT1A1}$ was estimated by dividing the reported IC_{50} value in half, assuming competitive inhibition. F_g, the fraction of substrate escaping gut-wall metabolism, was assumed to be 1 based on DTG's in vitro intrinsic clearance and high passive permeability. F_m is the fraction of the substrate dose metabolized by a specific enzyme (e.g., CYP3A4 or UGT1A1).

Results

ATP-binding Cassette (ABC) Transporter Substrate Assays. To determine whether [^{14}C]DTG is a substrate for human Pgp or BCRP, the in vitro bidirectional transport across MDCKII monolayers expressing these transporters was studied. In addition, the passive permeability was determined by inclusion of GF120918, a Pgp and BCRP inhibitor. The efflux ratio for [^{14}C]DTG across the MDCKII-MDR1 monolayers was 3.8 and decreased to 0.74 in the presence of GF120918, consistent with DTG being a substrate for Pgp (Table 1). For BCRP, the efflux ratio of [^{14}C]DTG across the MDCKII-BCRP monolayers was 3.1 and decreased to 0.80 in the presence of GF120918 (Table 1), consistent with DTG being a substrate for BCRP. The in vitro passive membrane permeability of [^{14}C]DTG across the MDCKII monolayers was 333 nm/s ($P_{7.4}$ B→A + GF120918) using Dulbecco's Modification of Eagle's Medium as the transport buffer, and was 265 ($P_{5.5[abs]}$) and 252 ($P_{7.4[abs]}$) nm/sec using fasted state simulated intestinal fluid (FaSSIF) buffer, at pH 5.5/7.4 (donor/receiver) and 7.4/7.4, respectively. These results demonstrate that DTG has high membrane permeability independent of pH.

ABC and Solute Carrier (SLC) Transporter Inhibition Assays. The inhibition of Pgp and BCRP by DTG was assessed by determining the B→A transport of [^{3}H]digoxin and [^{14}C]cimetidine across MDCKII-MDR1 or MDCKII-BCRP monolayers, respectively. DTG at a concentration of 100μM decreased the Pgp-mediated transport of [^{3}H]digoxin by 29%, and inhibited BCRP-mediated transport of [^{14}C]cimetidine by 43% at 30 μM and 50% at 100 μM. However, due to solubility limitations of DTG, an IC_{50} value could not be determined (Table 2). MRP2 inhibition by DTG and its ether glucuronide, M2, was assessed by measuring the uptake of [^{3}H]EG in MRP2 membrane vesicles. At all concentrations tested (0.1 to 100 μM), no

inhibition of [^{3}H]EG uptake in MRP2 vesicles was observed (IC_{50} >100μM; Table 2).

OATP1B1 and OATP1B3 inhibition by DTG was investigated by determining the uptake of [^{3}H]EG in CHO-OATP1B1 and HEK-MSRII-OATP1B3 cells, respectively. At all concentrations tested (0.3 to 100 μM), no discernable inhibition of [^{3}H]EG uptake by DTG was observed for OATP1B1 or OATP1B3 (IC_{50} >100μM; Table 2).

The inhibitory effect of DTG on human organic cation transporter 1 (OCT1) and 2 (OCT2) was investigated by measuring the uptake of [^{14}C]metformin in HEK293-OCT1 and MDCKII-OCT2 cells, respectively. DTG at 10μM slightly inhibited OCT1 transport by 22%. However, DTG notably inhibited the renal transporter OCT2 by 91% when tested at a concentration of 25μM. Based on this observation, a study to determine the IC_{50} value against OCT2 was completed. DTG inhibited OCT2 with an IC_{50} value of 1.9μM (Table 2, Figure 1).

Identification of Enzymes Responsible for the Metabolism of Dolutegravir. Using primary human hepatocytes, HLMs, and cDNA-expressed CYP and UGT enzymes, the products of [^{14}C]DTG metabolism and the relative contributions of the enzymes involved were defined. In human hepatocytes and UDPGA-fortified HLMs, the only metabolite of DTG observed was an ether glucuronide (M2). The ether glucuronide formation rate was highest in UGT1A1 incubations, with a much lower rate in UGT1A3 and 1A9 incubations (Figure 2A). M2 was not detected in vector control, UGT1A4, 1A6, 2B4, 2B7, or 2B15 incubations. The importance of UGT1A1 in [^{14}C]DTG metabolism was confirmed using atazanavir as a selective UGT1A1 inhibitor in UDPGA-fortified HLM incubations. Atazanavir potently inhibited the

DMD Fast Forward. Published on November 6, 2012 as DOI: 10.1124/dmd.112.048918
This article has not been copyedited and formatted. The final version may differ from this version.

glucuronidation of [^{14}C]DTG with a calculated IC_{50} value of 0.39μM (Figure 2B). Further studies were done to determine the formation kinetics of the DTG glucuronide. The estimated kinetic parameters, K_m, V_{max}, and CL_i, for M2 formation in HLM were 149μM, 409pmol/min/mg, and 2.7μL/min/mg, respectively (Figure 3A), and for the recombinant human UGT1A1 enzyme were 21μM, 67pmol/min/mg, and 3.2μL/min/mg, respectively (Figure 3B).

The oxidative metabolism of [^{14}C]DTG (5μM) was studied in NADPH-fortified HLM and recombinant CYP enzymes. An oxidative metabolite (M3) was formed in CYP3A4 incubations (Figure 2C) with an intrinsic clearance of 3.0 μL/min/mg. M3 was also observed in HLM incubations (Figure 2C) and its formation was completely inhibited by azamulin, a selective CYP3A4 inhibitor. In addition, an N-dealkylated metabolite (M1), which is a hydrolysis product of M3, was observed in the CYP3A4 incubations. No DTG metabolites were observed in CYP1A2, 2B6, 2C8, 2C9, 2C19, or 2D6 incubations indicating that CYP3A4 is the primary CYP enzyme involved in the oxidative metabolism of DTG in vitro. The overall metabolic profile for DTG is summarized in Figure 4.

CYP and UGT Inhibition by Dolutegravir. The inhibition of human CYP enzymes by DTG was evaluated using HLM and selective CYP probe substrates (Table 3). DTG inhibited CYP2B6, 2C9, 2C19, 2D6 and 3A4 (nifedipine), but the percentage of inhibition observed (range 20 to 40%) at the highest concentration tested (100μM) was weak and insufficient to calculate an IC_{50}. In contrast, DTG inhibited CYP3A4-mediated metabolism of atorvastatin with a calculated IC_{50} of 54μM (Table 3). DTG did not inhibit CYP1A2, 2A6, or 2C8 (IC_{50} >100μM; Table 3). CYP3A4 metabolism-dependent inhibition was observed for nifedipine and

atorvastatin with decreases in IC_{50} values following cofactor preincubation. DTG was not a metabolism-dependent inhibitor of CYP1A2, 2A6, 2B6, 2C8, 2C9, 2C19, or 2D6.

The inhibition of human UGT1A1 and 2B7 enzymes by DTG was evaluated by measuring the enzyme activities of scopoletin and 7-hydroxy-4-(trifluoromethyl) coumarin (7-HFC) in recombinant human UGT1A1 and 2B7 enzymes, respectively, using fluorescence detection. DTG was not an inhibitor of UGT2B7 at concentrations up to 100μM. Weak inhibition of UGT1A1 was observed; however, inhibition (33%) at the highest concentration tested was insufficient to calculate an IC_{50} value (IC_{50} >100μM).

CYP Induction by Dolutegravir. The potential of DTG to induce CYP1A2, 2B6, and 3A4 mRNA was assessed in primary cultured human hepatocytes using TaqMan™ technology. After incubation for 48 hours with DTG (1 to 40μM), there was no notable induction of CYP1A2, 2B6 or 3A4.

Discussion

The studies presented herein describe the in vitro disposition and metabolism of DTG and the potential for DTG to be a victim or perpetrator of DDIs via modulation of transporters or metabolizing enzymes. Like other antiretroviral agents, DTG will be co-administered in combination with a variety of other drugs. Therefore, assessment of potential DDIs is an essential aspect in the clinical development of DTG.

Based on the limited aqueous solubility and high permeability, DTG is a Biopharmaceutics Drug Disposition Classification System class 2 drug [Benet et al., 2011;Benet et al., 2008], where efflux transporters and metabolizing enzymes are predicted to be important in the drug's disposition. Indeed, in vitro studies show that DTG undergoes extensive metabolism and is a substrate for Pgp and BCRP, two transporters reported to influence the intestinal absorption and CNS penetration of HIV drugs [Kivisto et al., 2004]. Although DTG is a substrate for efflux transporters, it exhibits rapid oral absorption (T_{max} ~2hr following a 50mg dose) and displays dose proportional kinetics with low to moderate variability [Min et al., 2010]. These data suggest that the high intrinsic passive membrane permeability attenuates any impact efflux transporters may have on DTG's intestinal absorption in humans. This is further supported by clinical studies that have demonstrated no clinically significant change in DTG pharmacokinetics when co-administration with lopinavir/ritonavir [Song et al., 2011d], which are known Pgp and BCRP inhibitors.

In a human mass balance study where healthy subjects received 20 mg of [^{14}C]DTG, 31.6% of the total oral dose was excreted in the urine, represented mainly by an ether glucuronide (M2,

18.9% of total dose), N-dealkylation (M1, 3.6% of total dose), and a metabolite formed by oxidation at the benzylic carbon (M3, 3.0% of total dose) (GSK data on file). Fecal elimination contributed an additional 3.1%, resulting in approximately 10% of the metabolism of DTG being represented by oxidative products. Based on the fraction of the dose renally eliminated and the intrinsic clearance values determined from in vitro UGT and CYP3A4 studies, the fraction of DTG metabolized by UGT1A1 ($f_{mUGT1A1}$) and CYP3A4 ($f_{mCYP3A4}$) is estimated to be 0.51 and 0.21, respectively. The fraction of DTG metabolized by UGT1A3 and 1A9 is estimated at 0.028 and 0.055, respectively. It should be noted that the estimates of f_{mUGT} may be underestimated due to the instability of the ether glucuronide in feces, as the conjugate may hydrolyze and convert back to parent drug under these conditions. Since DTG is a substrate for UGT1A1 and CYP3A4, pharmacokinetic interactions involving co-administration of a UGT1A1 or CYP3A4 inhibitor or inducer could perturb the pharmacokinetics of DTG. Based on the fraction of DTG metabolized, an interaction with UGT1A1 and CYP3A4 inhibitors may be expected if both pathways are fully inhibited (combined $f_m = 0.72$). Ritonavir and atazanavir are HIV PIs that have been co-administered with DTG [Song et al., 2011a]. Both are potent CYP3A4 inhibitors and atazanavir is also a marked UGT1A1 inhibitor. Using a mechanistic static equation (see Materials and Methods) and the estimated f_m above, the AUC of DTG was expected to increase by as much as 1.8 to 2.0-fold when co-administered with ritonavir-boosted atazanavir. Indeed, when DTG was co-dosed with 400mg atazanavir in a clinical study, there was a 1.9- and 1.5-fold increase in DTG $AUC_{(0-t)}$ and C_{max}, respectively [Song et al., 2011a]. When dosed with atazanavir/ritonavir (300/100mg), the DTG $AUC_{(0-t)}$ and C_{max} increased 1.62-fold and 1.34-fold. These data are consistent with UGT1A1 and CYP3A4 being the important

pathways of DTG metabolism in vivo, with UGT1A3 and UG1A9 having minor roles in DTG clearance.

In contrast to inhibition of metabolic pathways, metabolic inducers such as rifampin, etravirine, efavirenz and tipranavir need to be considered as they are important agents in the treatment of HIV and other infectious diseases. It is also known that strong activators of human PXR can lead to increased metabolic activity for UGT1A1, CYP3A4 and transporters [Chen et al., 2012]. Induction of these pathways could increase the systemic clearance of DTG resulting in lower exposures. Both etravirine and efavirenz reduce the $AUC_{(0-t)}$ of DTG by 71% and 57%, respectively [Song et al., 2011c;Song et al., 2011b]. This interaction with DTG is likely the combined effect of UGT and CYP3A4 induction. This is consistent with etravirine and efavirenz causing modest decreases (20 to 40%) in the pharmacokinetics of raltegravir, a sensitive UGT substrate [Kassahun et al., 2007;Iwamoto et al., 2008]. Support for a role of CYP3A4 induction was demonstrated by co-administration of the potent CYP3A4 inhibitors lopinavir/ritonavir or darunavir/ritonavir that counteracted the decrease in DTG exposure by etravirine [Song et al., 2011c]. Alternatively, the decreases in DTG exposure could also involve drug transporters. One interesting possibility is (modest) MRP2 inhibition leading to a partial disruption in the enterohepatic recirculation of DTG; both etravirine and efavirenz are inhibitors of MRP2 [Zembruski et al., 2011b]. This has been reported as an explanation for the reduced exposure of mycophenolate mofetil when co-dosed with cyclosporine A [Hesselink et al., 2005].

At clinically relevant concentrations, DTG does not result in drug interactions by inhibition or induction of CYP enzymes, or UGT1A1/2B7 inhibition. Although DTG demonstrated weak

CYP3A4 metabolism-dependent inhibition of nifedipine and atorvastatin in vitro (approximately 1.6 fold reduction in IC_{50}; Table 3), a clinical study demonstrated that DTG had no effect on midazolam's pharmacokinetics [Min et al., 2010], confirming that DTG does not inhibit or induce CYP3A4 in vivo.

The DTG IC_{50} values for all transporters examined were >30μM except for OCT2 (discussed below). These IC_{50} values are higher than the peak plasma concentration of DTG following a 50 mg daily dose (3.45 μg/mL, ~8μM) [Song et al., 2010], supporting the overall low potential for transporter-mediated drug interactions ($[I_{1,total}]/IC_{50}$; Table 2) [Giacomini et al., 2010;Zhang et al., 2008]. Further, the overall drug interaction risk is even lower due to the high plasma protein binding (>99%) of DTG (GSK data on file). Finally, calculation of inhibition of efflux transporters in the intestine following a 50 mg dose supports a limited risk of DDIs as the $[I_2]/IC_{50}$ values for both Pgp and MRP2 are below 5 (Table 2) [Zhang et al., 2008;Giacomini et al., 2010]. However, based on the $[I_2]/IC_{50}$ value for BCRP likely being close to 10, there could be a small risk of inhibition of this transporter by DTG. Our findings are consistent with in vitro data reported by Lepist et al. indicating that DTG is a weak or non-inhibitor of Pgp (IC_{50s} > 90μM), MRP2 (IC_{50s} > 90μM), and BCRP (IC_{50} = 67μM) [Lepist et al., 2011]. Overall, the data support a low potential for DTG to cause clinically significant DDIs with other drugs such as simvastatin, rosuvastatin and atorvastatin (OATP, BCRP and CYP substrates), and metformin (OCT1/2 substrate). A clinical study with tenofovir, an OAT and MRP4 substrate [Ray et al., 2006], demonstrated no interaction of DTG on tenofovir pharmacokinetics [Song et al., 2010], suggesting that DTG is not an inhibitor of these transporters in vivo.

In contrast to the other transporters discussed, DTG causes notable in vitro inhibition of the renal transporter OCT2 (IC_{50} = 1.9μM). As this value is 4-fold lower than the C_{max} of DTG ($[I_{1,total}]/IC_{50}$=4.2), a potential interaction exists for compounds that undergo renal secretion via OCT2, such as circulating serum creatinine (a product of muscle turnover) and the anti-arrhythmic drug dofetilide. The in vitro OCT2 inhibition data are consistent with the mild 10-14% decreases in serum creatinine clearanceobserved in patients administered DTG [Koteff et al., 2011;vanLunzen et al., 2012]. These mild, reversible changes are similar to other clinical observations with OCT/MATE inhibitors such as dronedarone, AZD0837, and DX-619 [Tschuppert et al., 2007;Schutzer et al., 2010;Sarapa et al., 2007;Imamura et al., 2011]. A clinical study confirmed that the changes in creatinine were not due to DTG altering renal blood flow or renal clearance; therefore, the changes in creatinine serum levels are likely due to the inhibition of the OCT2 transporter [Koteff et al., 2011;Schutzer et al., 2010;Kusuhara et al., 2011]. Caution with concomitant dosing of DTG and dofetilide, a narrow therapeutic index class III anti-arrhythmic agent, is warranted as OCT2 inhibition can significantly reduce its renal clearance as shown by a clinical interaction with cimetidine [Roukoz and Saliba, 2007]. However, there is less concern for other OCT substrates, such as metformin, as these drugs have larger therapeutic windows compared to dofetilide. In addition, the lack of significant inhibition of OCT1 allows transport of metformin to the liver, its site of action, to maintain its pharmacological effect.

In conclusion, these in vitro studies reveal the low propensity of DTG to cause drug interactions through metabolic or transporter pathways, consistent with the lack of clinical interactions observed to date with DTG. Further, these studies provide a mechanistic explanation for the

DDIs observed with DTG when co-administered with CYP, UGT and transporter inhibitors and/or inducers. As a result of the multiple clearance pathways of DTG, few clinically significant alterations in DTGs pharmacokinetics have been observed that require a dose adjustment. This is consistent with the current safety profile of DTG in humans.

Acknowledgements

The authors wish to thank Jane Rosemond, Jim Bishop, Masuma Naqwe, John Ulrich, Jo Salisbury and Lindsey Harston for their technical support and Gary Bowers for review of this manuscript and to colleagues at GlaxoSmithKline who encouraged and supported this study.

Author contributions

Participated in research design: Reese, Savina, Tracey, Generaux, Humphreys, Clarke, Kanaoka, Webster, Harmon, and Polli

Conducted experiments: Reese, Humphreys, Tracey, Webster, Clarke, Harmon, and Generaux,

Performed data analysis: Reese, Savina, Generaux, Humphreys, Tracey, Webster, Clarke, Harmon, and Polli

Wrote or contributed to the writing of the manuscript: Reese, Savina, Generaux, Tracey, Kanaoka and Polli

Reference List

Benet LZ, Amidon GL, Barends DM, Lennernas H, Polli JE, Shah VP, Stavchansky SA, and Yu LX (2008) The use of BDDCS in classifying the permeability of marketed drugs. *Pharm Res* **25:**483-488.

Benet LZ, Broccatelli F, and Oprea TI (2011) BDDCS applied to over 900 drugs. *AAPS J* **13:**519-547.

Bowen WP, Carey JE, Miah A, McMurray HF, Munday PW, James RS, Coleman RA, and Brown AM (2000) Measurement of cytochrome P450 gene induction in human hepatocytes using quantitative real-time reverse transcriptase-polymerase chain reaction. *Drug Metab Dispos* **28:**781-788.

Busti AJ, Hall RG, and Margolis DM (2004) Atazanavir for the treatment of human immunodeficiency virus infection. *Pharmacotherapy* **24:**1732-1747.

Chen Y, Tang Y, Guo C, Wang J, Boral D, and Nie D (2012) Nuclear receptors in the multidrug resistance through the regulation of drug-metabolizing enzymes and drug transporters. *Biochem Pharmacol* **83:**1112-1126.

Collier AC, Tingle MD, Keelan JA, Paxton JW, and Mitchell MD (2000) A highly sensitive fluorescent microplate method for the determination of UDP-glucuronosyl transferase activity in tissues and placental cell lines. *Drug Metab Dispos* **28:**1184-1186.

Dixit V, Hariparsad N, Li F, Desai P, Thummel KE, and Unadkat JD (2007) Cytochrome P450 enzymes and transporters induced by anti-human immunodeficiency virus protease inhibitors in human hepatocytes: implications for predicting clinical drug interactions. *Drug Metab Dispos* **35:**1853-1859.

Evans DF, Pye G, Bramley R, Clark AG, Dyson TJ, and Hardcastle JD (1988) Measurement of gastrointestinal pH profiles in normal ambulant human subjects. *Gut* **29:**1035-1041.

Giacomini KM, Huang SM, Tweedie DJ, Benet LZ, Brouwer KL, Chu X, Dahlin A, Evers R, Fischer V, Hillgren KM, Hoffmaster KA, Ishikawa T, Keppler D, Kim RB, Lee CA, Niemi M, Polli JW, Sugiyama Y, Swaan PW, Ware JA, Wright SH, Yee SW, Zamek-Gliszczynski MJ, and Zhang L (2010) Membrane transporters in drug development. *Nat Rev Drug Discov* **9:**215-236.

Granfors MT, Wang JS, Kajosaari LI, Laitila J, Neuvonen PJ, and Backman JT (2006) Differential inhibition of cytochrome P450 3A4, 3A5 and 3A7 by five human immunodeficiency virus (HIV) protease inhibitors in vitro. *Basic Clin Pharmacol Toxicol* **98:**79-85.

Hariparsad N, Nallani SC, Sane RS, Buckley DJ, Buckley AR, and Desai PB (2004) Induction of CYP3A4 by efavirenz in primary human hepatocytes: comparison with rifampin and phenobarbital. *J Clin Pharmacol* **44:**1273-1281.

Hesselink DA, van Hest RM, Mathot RA, Bonthuis F, Weimar W, de Bruin RW, and van Gelder

T (2005) Cyclosporine interacts with mycophenolic acid by inhibiting the multidrug resistance-associated protein 2. *Am J Transplant* **5:**987-994.

Hilgendorf C, Ahlin G, Seithel A, Artursson P, Ungell AL, and Karlsson J (2007) Expression of thirty-six drug transporter genes in human intestine, liver, kidney, and organotypic cell lines. *Drug Metab Dispos* **35:**1333-1340.

Hinton LK, Galetin A, and Houston JB (2008) Multiple inhibition mechanisms and prediction of drug-drug interactions: status of metabolism and transporter models as exemplified by gemfibrozil-drug interactions. *Pharm Res* **25:**1063-1074.

Hull MW and Montaner JS (2011) Ritonavir-boosted protease inhibitors in HIV therapy. *Ann Med* **43:**375-388.

Imamura Y, Murayama N, Okudaira N, Kurihara A, Okazaki O, IzumiT, Inoue K, Yuasa H, Kusuhara H and Sugiyama Y (2011) Prediction of fluoroquinolone-induced elevation in serum creatinine levels: a case of drug-endogenous substance interaction involving the inhibition of renal secretion. *Clin Pharmacol Ther* **89;**81–88.

Ito K, Iwatsubo T, Kanamitsu S, Nakajima Y, and Sugiyama Y (1998) Quantitative prediction of in vivo drug clearance and drug interactions from in vitro data on metabolism, together with binding and transport. *Annu Rev Pharmacol Toxicol* **38:**461-499.

Iwamoto M, Wenning LA, Petry AS, Laethem M, De SM, Kost JT, Breidinger SA, Mangin EC, Azrolan N, Greenberg HE, Haazen W, Stone JA, Gottesdiener KM, and Wagner JA (2008) Minimal effects of ritonavir and efavirenz on the pharmacokinetics of raltegravir. *Antimicrob Agents Chemother* **52:**4338-4343.

Kassahun K, McIntosh I, Cui D, Hreniuk D, Merschman S, Lasseter K, Azrolan N, Iwamoto M, Wagner JA, and Wenning LA (2007) Metabolism and disposition in humans of raltegravir (MK-0518), an anti-AIDS drug targeting the human immunodeficiency virus 1 integrase enzyme. *Drug Metab Dispos* **35:**1657-1663.

Kivisto KT, Niemi M, and Fromm MF (2004) Functional interaction of intestinal CYP3A4 and P-glycoprotein. *Fundam Clin Pharmacol* **18:**621-626.

Koteff J, Borland J, Chen S, Song I, Peppercorn A, Koshiba T, Cannon C, Muster H, and Piscitelli SC (2011) An open label, placebo-controlled study to evaluate the effect of dolutegravir (DTG, S/GSK1349572) on iohexol and para-aminohippurate clearance in healthy subjects. 51st Interscience Conference on Antimicrobial Agents and Chemotherapy (ICAAC) 51.

Kusuhara H, Ito S, Kumagai Y, Jiang M, Shiroshita T, Moriyama Y, Inoue K, Yuasa H, and Sugiyama Y (2011) Effects of a MATE protein inhibitor, pyrimethamine, on the renal elimination of metformin at oral microdose and at therapeutic dose in healthy subjects. *Clin Pharmacol Ther* **89:**837-844.

Lepist EI, Murray BP, Tong L, Roy A, Bannister R, and Ray AS (2011) Effect of cobicistat and ritonavir on proximal renal tubular cell uptake and efflux transporters. Antimicrobial Agents and

Chemotherapy , A1-1724.

Lui CY, Amidon GL, Berardi RR, Fleisher D, Youngberg C, and Dressman JB (1986) Comparison of gastrointestinal pH in dogs and humans: implications on the use of the beagle dog as a model for oral absorption in humans. *J Pharm Sci* **75:**271-274.

Min S, Song I, Borland J, Chen S, Lou Y, Fujiwara T, and Piscitelli SC (2010) Pharmacokinetics and safety of S/GSK1349572, a next-generation HIV integrase inhibitor, in healthy volunteers. *Antimicrob Agents Chemother* **54:**254-258.

Mukwaya G, MacGregor T, Hoelscher D, Heming T, Legg D, Kavanaugh K, Johnson P, Sabo JP, and McCallister S (2005) Interaction of ritonavir-boosted tipranavir with loperamide does not result in loperamide-associated neurologic side effects in healthy volunteers. *Antimicrob Agents Chemother* **49:**4903-4910.

Palella FJ, Jr., Baker RK, Moorman AC, Chmiel JS, Wood KC, Brooks JT, and Holmberg SD (2006) Mortality in the highly active antiretroviral therapy era: changing causes of death and disease in the HIV outpatient study. *J Acquir Immune Defic Syndr* **43:**27-34.

Palella FJ, Jr., Delaney KM, Moorman AC, Loveless MO, Fuhrer J, Satten GA, Aschman DJ, and Holmberg SD (1998) Declining morbidity and mortality among patients with advanced human immunodeficiency virus infection. HIV Outpatient Study Investigators. *N Engl J Med* **338:**853-860.

Panel on Antiretroviral Guidelines for Adults and Adolescents (2012) Guidelines for the Use of Antiretroviral Agents in HIV-1-Infected Adults and Adolescents. *Department of Health and Human Services*, 1-161.

Polli JW, Humphreys JE, Harmon KA, Castellino S, O'Mara MJ, Olson KL, John-Williams LS, Koch KM, and Serabjit-Singh CJ (2008) The role of efflux and uptake transporters in [N-{3-chloro-4-[(3-fluorobenzyl)oxy]phenyl}-6-[5-({[2-(methylsulfonyl)ethyl]amino }methyl)-2-furyl]-4-quinazolinamine (GW572016, lapatinib) disposition and drug interactions. *Drug Metab Dispos* **36:**695-701.

Polli JW, Hussey E, Bush M, Generaux GT, Smith G, Collins D, McMullen S, Turner N, and Nunez DJ (2012) Evaluation of Drug Interactions of GSK1292263 (a GPR119 Agonist) with Statins: From In Vitro Data to Clinical Study Design. *Xenobiotica* (in press).

Polli JW, Wring SA, Humphreys JE, Huang L, Morgan JB, Webster LO, and Serabjit-Singh CS (2001) Rational use of in vitro P-glycoprotein assays in drug discovery. *J Pharmacol Exp Ther* **299**:620-628.

Rautio J, Humphreys JE, Webster LO, Balakrishnan A, Keogh JP, Kunta JR, Serabjit-Singh CJ, and Polli JW (2006) In vitro p-glycoprotein inhibition assays for assessment of clinical drug interaction potential of new drug candidates: a recommendation for probe substrates. *Drug Metab Dispos* **34:**786-792.

Ray AS, Cihlar T, Robinson KL, Tong L, Vela JE, Fuller MD, Wieman LM, Eisenberg EJ, and

Rhodes GR (2006) Mechanism of active renal tubular efflux of tenofovir. *Antimicrob Agents Chemother* **50:**3297-3304.

Roukoz H and Saliba W (2007) Dofetilide: a new class III antiarrhythmic agent. *Expert Rev Cardiovasc Ther* **5:**9-19.

Sarapa N, Wickremasingha P, Ge N, Weitzman R, Fuellhart M, Yen C, and Lloyd-Parks J (2007) Lack of effect of DX-619, a novel des-fluoro(6)-quinolone, on glomerular filtration rate measured by serum clearance of cold iohexol. *Antimicrob Agents Chemother* **51:**1912-1917.

Schutzer KM, Svensson MK, Zetterstrand S, Eriksson UG, and Wahlander K (2010) Reversible elevations of serum creatinine levels but no effect on glomerular filtration during treatment with the direct thrombin inhibitor AZD0837. *Eur J Clin Pharmacol* **66:**903-910.

Song I, Borland J, Chen S, Lou Y, Peppercorn A, Wajima T, Min S, and Piscitelli SC (2011a) Effect of atazanavir and atazanavir/ritonavir on the pharmacokinetics of the next-generation HIV integrase inhibitor, S/GSK1349572. *Br J Clin Pharmacol* **72:**103-108.

Song I, Borland J, Lou Y, Chen S, Patel P, Guta P, Wajima T, Peppercorn A, and Piscitelli SC (2011b) Effects of enzyme inducers, tipranavir and efavirenz, on the pharmacokinetics of the integrase inhibitor, dolutegravir (S/GSK1349572). 12th International Workshop on Clinical Pharmacology of HIV Therapy (O_02).

Song I, Borland J, Min S, Lou Y, Chen S, Patel P, Wajima T, and Piscitelli SC (2011c) Effects of etravirine alone and with ritonavir-boosted protease inhibitors on the pharmacokinetics of dolutegravir. *Antimicrob Agents Chemother* **55:**3517-3521.

Song I, Min SS, Borland J, Lou Y, Chen S, Ishibashi T, Wajima T, and Piscitelli SC (2010) Lack of interaction between the HIV integrase inhibitor S/GSK1349572 and tenofovir in healthy subjects. *J Acquir Immune Defic Syndr* **55:**365-367.

Song I, Min SS, Borland J, Lou Y, Chen S, Patel P, Ishibashi T, and Piscitelli SC (2011d) The effect of lopinavir/ritonavir and darunavir/ritonavir on the HIV integrase inhibitor S/GSK1349572 in healthy participants. *J Clin Pharmacol* **51:**237-242.

Tschuppert Y, Buclin T, Rothuizen LE, Decosterd LA, Galleyrand J, Gaud C, and Biollaz J (2007) Effect of dronedarone on renal function in healthy subjects. *Br J Clin Pharmacol* **64:**785-791.

van Lunzen J, Maggiolo F, Arribas JR, Rakhmanova A, Yeni P, Young B, Rockstroh JK, Almond S, Song I, Brothers C, and Min S (2012) Once daily dolutegravir (S/GSK1349572) in combination therapy in antiretroviral-naive adults with HIV: planned interim 48 week results from SPRING-1, a dose-ranging, randomised, phase 2b trial. *Lancet Infect Dis* **12:**111-118.

Yanakakis LJ and Bumpus NN (2012) Biotransformation of the antiretroviral drug etravirine: metabolite identification, reaction phenotyping, and characterization of autoinduction of cytochrome P450-dependent metabolism. *Drug Metab Dispos* **40:**803-814.

Yeh RF, Gaver VE, Patterson KB, Rezk NL, Baxter-Meheux F, Blake MJ, Eron JJ, Jr., Klein CE, Rublein JC, and Kashuba AD (2006) Lopinavir/ritonavir induces the hepatic activity of cytochrome P450 enzymes CYP2C9, CYP2C19, and CYP1A2 but inhibits the hepatic and intestinal activity of CYP3A as measured by a phenotyping drug cocktail in healthy volunteers. *J Acquir Immune Defic Syndr* **42:**52-60.

Zembruski NC, Buchel G, Jodicke L, Herzog M, Haefeli WE, and Weiss J (2011a) Potential of novel antiretrovirals to modulate expression and function of drug transporters in vitro. *J Antimicrob Chemother* **66:**802-812.

Zembruski NC, Haefeli WE, and Weiss J (2011b) Interaction potential of etravirine with drug transporters assessed in vitro. *Antimicrob Agents Chemother* **55:**1282-1284.

Zhang D, Chando TJ, Everett DW, Patten CJ, Dehal SS, and Humphreys WG (2005) In vitro inhibition of UDP glucuronosyltransferases by atazanavir and other HIV protease inhibitors and the relationship of this property to in vivo bilirubin glucuronidation. *Drug Metab Dispos* **33:**1729-1739.

Zhang L, Zhang YD, Strong JM, Reynolds KS, and Huang SM (2008) A regulatory viewpoint on transporter-based drug interactions. *Xenobiotica* **38:**709-724.

Footnotes

These studies were funded by GlaxoSmithKline, Shionogi & Co. Ltd. and ViiV Healthcare.

Legends for Figures:

Figure 1. The effect of DTG on human OCT2 transport in vitro. The inhibition of OCT2 by DTG (concentration range 0.1 to 30 μM) was investigated by determining the uptake of [^{14}C]-metformin in MDCKII-OCT2 cells. Data are the mean (± standard deviation) from triplicate wells.

Figure 2. Formation of DTG metabolites by recombinant human CYP and UGT enzymes. (A) Formation of DTG glucuronide metabolite (M2) in UDPGA-fortified recombinant human UGT enzyme and HLM incubations. [^{14}C]DTG (16 μM) incubated for 120 min at 1 mg/mL HLM protein. (B) Effect of atazanavir on [^{14}C]DTG glucuronidation in UDPGA-fortified HLM. [^{14}C]DTG (10 μM) was incubated with HLM (1 mg/mL protein) for 120 min. (C) M1 and M3 formation in NADPH-fortified human CYP enzyme and HLM incubations. [^{14}C]DTG (5 μM) was incubated for 120 minutes with 150 pmol/mL CYP enzyme or 2 mg/mL HLM.

Figure 3. Michaelis-Menten kinetic plots for DTG glucuronidation. (A) HLM and (B) human UGT1A1 enzyme incubations were conducted for 120 minutes with 1 mg/mL microsomal protein. Single incubations were run for 25 and 50 μM concentrations of DTG in UGT1A1 incubations only.

Figure 4. Metabolic Scheme of Dolutegravir.

Table 1: Results of Transport Studies for [^{14}C]-DTG (3 μM) in MDCKII-MDR1 or MDCKII-BCRP Cell Monolayers[a]

MDCKII Cell Line	GF120918[b]	Rate A→B (pmol/min/cm^2)	Rate B→A (pmol/min/cm^2)	Apical Efflux Ratio	A→B Mass Balance (%)	B→A Mass Balance (%)
MDR1	-	7.3 ± 0.52	28 ± 3.1	3.8	84 ± 7.1	84 ± 4.5
MDR1	+	4.7 ± 0.04	3.5 ± 0.07	0.74	84 ± 1.9	75 ± 1.7
BCRP	-	2.5 ± 0.24	7.8 ± 0.29	3.1	81 ± 3.4	85 ± 3.5
BCRP	+	4.2 ± 0.09	3.3 ± 0.06	0.80	81 ± 2.1	76 ± 2.4

[a] Data are the mean ± standard deviation from three monolayers over 90 min using Dulbecco's Modification of Eagle's Medium as the transport buffer. All donor compartments contained Lucifer yellow (100 μM) to determine monolayer integrity (pass criterion P 7.4 ≤50 nm/s). Amprenavir served as a positive control for Pgp efflux and cimetidine for BCRP efflux. The measured radiochemical purity of [^{14}C]-DTG was >98% and no metabolic or chemical degradation was detected during the studies.

[b] GF120918 was used in both donor and receiver compartments at 2 μM for Pgp and BCRP.

Table 2. Inhibition of Human ABC Transporters and Solute Carriers by DTG

Transporter	IC_{50} (μM)	Substrate	$[I_1]/IC_{50}$ [a]	$[I_2]/IC_{50}$ [b]
Pgp	>100	[^{3}H]-Digoxin	<0.08	<5
BCRP	>30	[^{14}C]cimetidine	<0.26*	<16**
OATP1B1	>100	[^{3}H]-estradiol 17β-D-glucuronide	<0.08	n/a [d]
OATP1B3	>100	[^{3}H]-estradiol 17β-D-glucuronide	<0.08	n/a
MRP2	>100	[^{3}H]-estradiol 17β-D-glucuronide	<0.08	<5
OCT1	NC[c]	[^{14}C]-Metformin	NC	NC
OCT2	1.9 (0.29)[d]	[^{14}C]-Metformin	4.2*	n/a

[a] $[I_1]$=8μM with DTG clinical daily dose of 50mg [Song et al., 2010]; *: possible DDI risk based on $[I_1]$>0.1 assuming $[I_1]$= total plasma concentration as described in [Zhang et al., 2008;Giacomini et al., 2010].

[b] $[I_2]$=477μM using 250mL gastrointestinal volume. **: possible DDI risk based on $[I_2]$>10 as described in [Zhang et al., 2008;Giacomini et al., 2010]

[c] Not calculated; DTG at a concentration of 10 μM inhibited OCT1 by 22%.

[d] n/a = not applicable; transporter not (highly) expressed in the gastrointestinal tract [Hilgendorf et al., 2007]

Table 3. Inhibition of CYP Enzymes by DTG in Human Liver Microsomes

CYP	Substrate	Metabolism-Dependent Inhibition		
		Control pre-incubation [a] IC_{50} (μM) [c]	NADPH pre-incubation [b] IC_{50} (μM)	Fold Change in IC_{50}
1A2	Phenacetin	>100	>100	NC
2A6	Coumarin	>100	>100	NC
2B6	Bupropion	>100 [d]	>100	NC
2C8	Rosiglitazone	>100	>100	NC
2C9	Diclofenac	>100 [d]	>100	NC
2C19	S-Mephenytoin	>100 [d]	>100	NC
2D6	Bufuralol	>100 [d]	>100	NC
3A4	Atorvastatin	54	33	1.6
3A4	Nifedipine	>100 [d]	65	>1.5

[a] Microsomes (0.1 mg/mL), buffer and DTG pre-incubated for 20 minutes with probe substrate prior to initiation of reaction with NADPH.
[b] Microsomes (0.1 mg/mL), buffer and DTG pre-incubated for 20 minutes with NADPH prior to initiation of reaction with probe substrate.
[c] Control pre-incubation IC_{50} = direct inhibition IC_{50}
[d] CYP inhibition was observed but the percentage of inhibition at the highest DTG concentration tested (100μM) was weak (20 to 40%) and insufficient to calculate an IC_{50}

NC: Not calculated

Figure 1

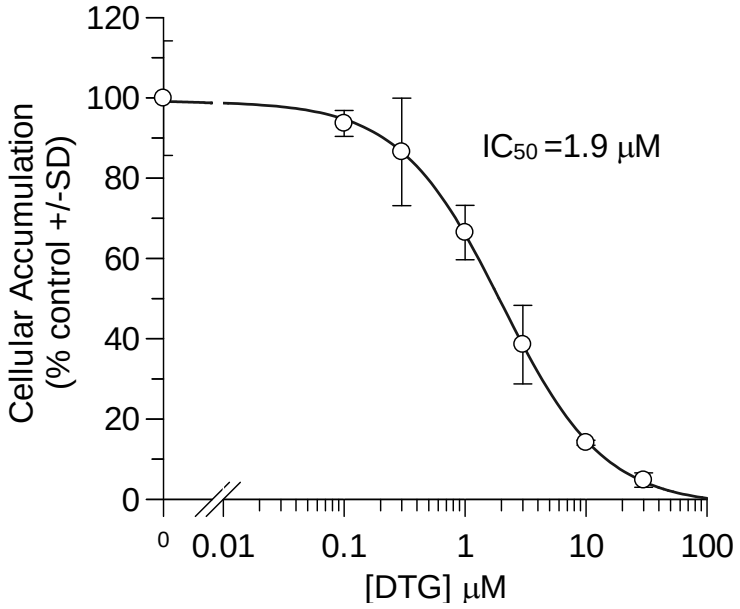

Figure 2

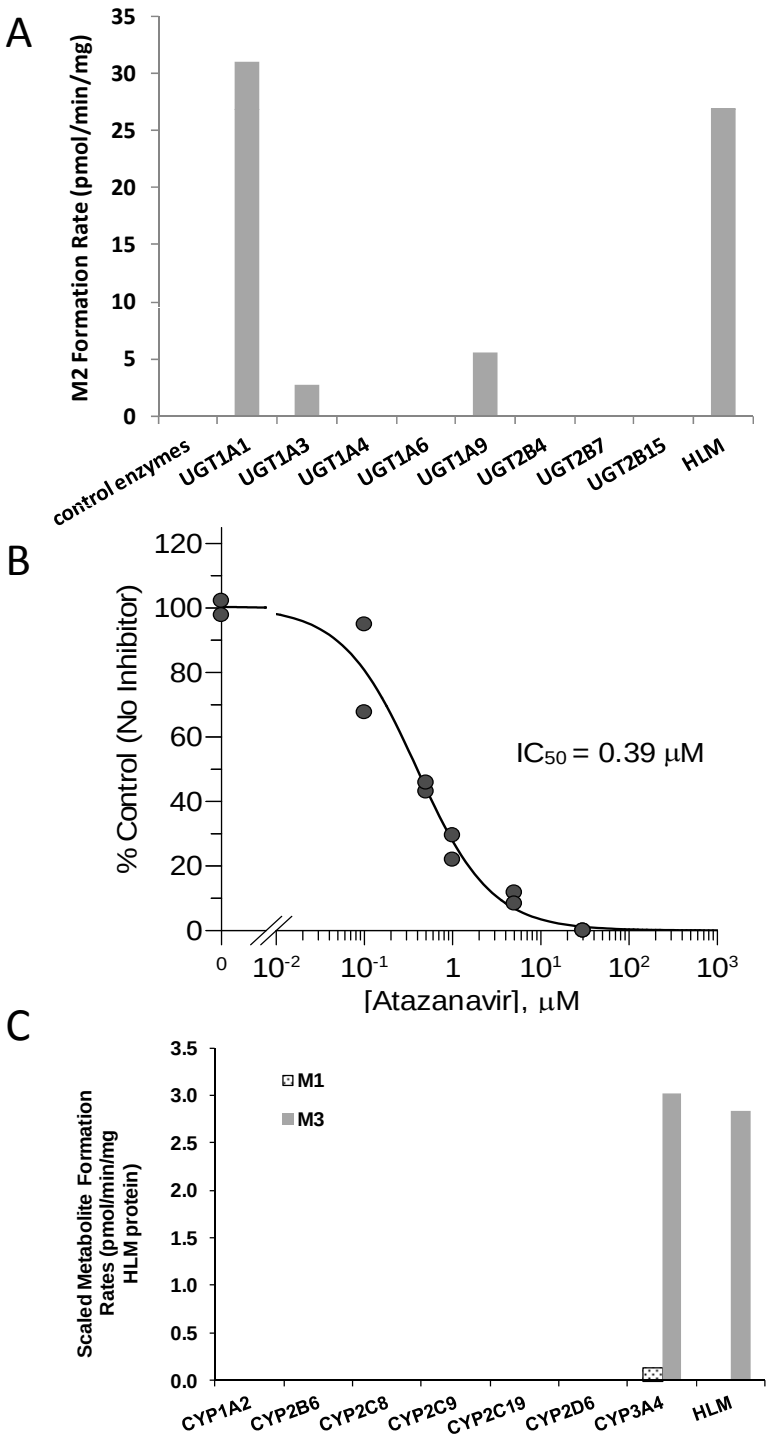

Figure 3

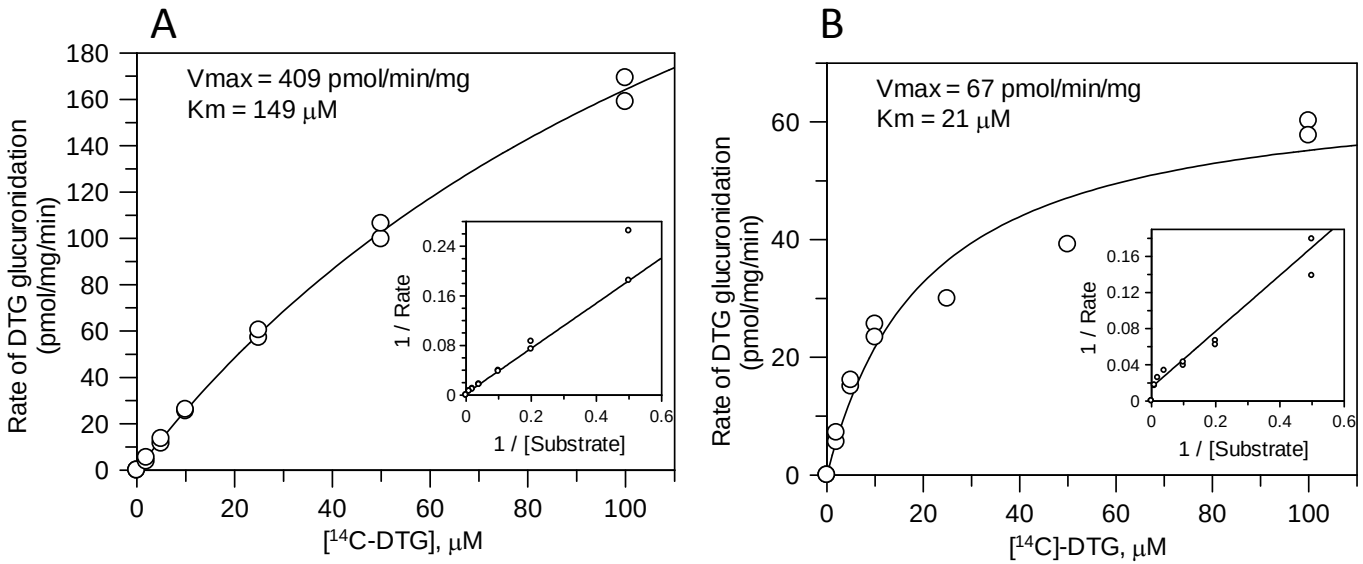

Figure 4